Available online at www.sciencedirect.com
SCIENCE DIRECT®
Bioorganic & Medicinal Chemistry 12 (2004) 5845–5856
Bioorganic & Medicinal Chemistry

Synthesis and evaluation of *N*-aryl and *N*-alkenyl CBI derivatives

Jay P. Parrish, John D. Trzupek, Terry V. Hughes, Inkyu Hwang and Dale L. Boger*

Department of Chemistry and the Skaggs Institute for Chemical Biology, The Scripps Research Institute, 10550 North Torrey Pines Road, La Jolla, CA 92037, USA

Received 20 July 2004; revised 23 August 2004; accepted 23 August 2004
Available online 15 September 2004

Abstract—The preparation of a novel series of *N*-aryl CBI derivatives in which an aryl substituent could be used to predictably modulate the reactivity of the resulting CC-1065/duocarmycin alkylation subunit analogue is detailed and its extension to a unique series of *N*-alkenyl derivatives is reported. The *N*-aryl derivatives were found to be exceptionally stable and to exhibit well-defined relationships between structure (X-ray), reactivity, and cytotoxic potency. When combined with the results of past investigations, the studies define a fundamental parabolic relationship between reactivity and cytotoxic potency. The parabolic relationship establishes that compounds in the series should possess sufficient stability to reach their biological target (DNA), yet maintain sufficient reactivity to effectively alkylate DNA upon reaching the biological target. Just as importantly, it defined this optimal balance of stability and reactivity that may be used for future design of related analogues. Notably, the duocarmycin SA and yatakemycin alkylation subunit lies at this optimal stability/reactivity position, whereas the CC-1065 and duocarmycin A alkylation subunits lie progressively and significantly to the left of this optimal position (too reactive).

1. Introduction

CC-1065 (**1**),[1] the duocarmycins (**2** and **3**),[2,3] and yatakemycin (**4**)[4] are the parent members of a class of potent antitumor agents whose properties originate from a now characteristic sequence-selective DNA alkylation (Fig. 1).[5–7] In the intervening years since their disclosures, extensive studies have defined structural features contributing to their DNA alkylation reaction and have established important relationships between structure and activity.[5–10]

The synthesis of analogues of **1**–**4** containing key structural changes in the alkylation subunits have been central to these studies providing insights not accessible through examination of the natural products themselves.[11] Among those introduced, the 1,2,9,9a-tetrahydrocyclopropa[*c*]benz[*e*]indol-4-one (CBI) alkylation subunit has emerged as one of the most extensively examined series (Fig. 2).[12] Herein, we report full details of the preparation and examination of a novel series of N^2-aryl derivatives of CBI in which the electronic properties of the aryl substituent could be systematically varied to predictably alter the reactivity,[13] and the extension of these studies to the examination of an additional unique series of *N*-alkenyl CBI derivatives. As detailed below, the *N*-aryl derivatives proved to be remarkably stable relative to the typical *N*-acyl derivatives and exhibited a direct correlation between reactivity and biological potency. When combined with the results of preceding studies, this series served to complete a well-defined parabolic relationship between reactivity and activity.

2. Results and discussion

2.1. Synthesis of *N*-aryl CBI derivatives

The *N*-aryl derivatives were prepared using a Buchwald–Hartwig[14] Pd(0)-catalyzed or Barton[15] Cu(II)-catalyzed N-arylation of CBI (**5**, Scheme 1), enlisting precursor aryl chlorides or triarylbismuthines, respectively. The former provided effective couplings with the electron-deficient aryl chlorides affording **12**–**15** (0.05 equiv $Pd_2(dba)_3$, 0.1 equiv $(Cy)_2P(DMAbp)$,[16] 1.6 equiv Cs_2CO_3, THF, reflux, 3–6 h, 53–96%), but failed to provide products with electron-rich aryl halides under the conditions examined. In these instances, the Cu(II)-catalyzed coupling of **5** with the triarylbismuthines[17] (1.1 equiv $Cu(OAc)_2$, 1.0 equiv Et_3N, CH_2Cl_2, 25 °C, 24–36 h, 39–64%) provided **6**–**11** in good

Keywords: CC-1065; Duocarmycins; Antitumor.
* Corresponding author. Tel.: +1 858 784 7522; fax: +1 858 784 7550; e-mail: boger@scripps.edu

0968-0896/$ - see front matter © 2004 Elsevier Ltd. All rights reserved.
doi:10.1016/j.bmc.2004.08.032

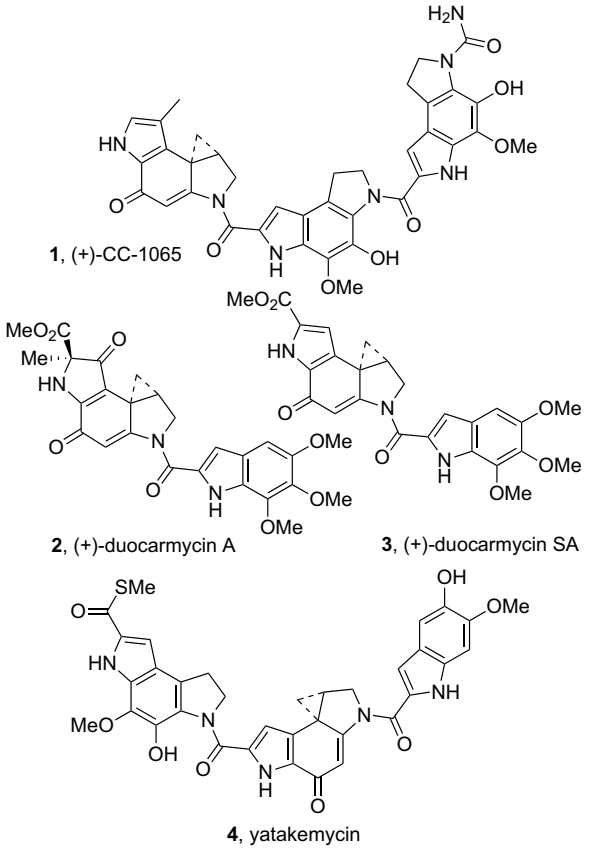

Figure 1.

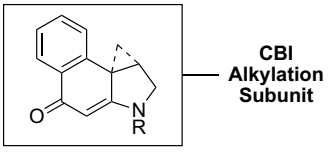

Figure 2.

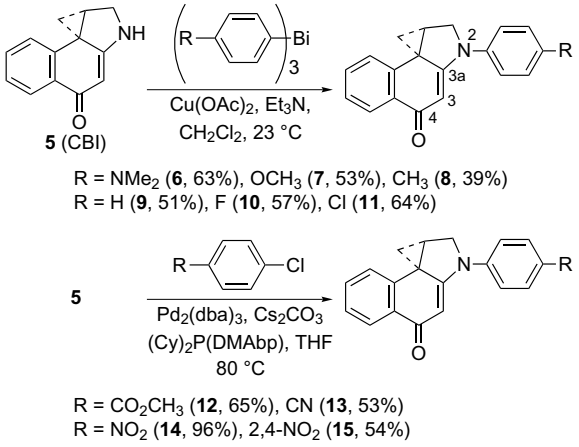

Scheme 1.

conversions. In the case of the Barton N-arylation, trace C3-arylation was also occasionally detected (5–10%).

2.2. Synthesis of *N*-alkenyl CBI derivatives

The coupling reaction was extended to a unique series of *N*-alkenyl CBI derivatives bearing a vinylogous enamide structure capped with a terminal aryl group. This included **17** incorporating a *p*-nitrophenyl group, which proved to be the most potent member of the *N*-aryl CBI derivatives, **18** bearing the appropriately substituted trimethoxyphenyl group to mimic the duocarmycin trimethoxyindole, and **20** incorporating the entire intact trimethoxyindole. The *N*-alkenyl derivatives were prepared using a Pd(0)-catalyzed N-vinylation reaction. Accordingly, the required 1,2-disubstituted bromoolefins were prepared from the corresponding aldehydes by the Corey–Fuchs reaction ($Ph_3P{=}CBr_2$)[18] followed by selective monodebromination (conditions for the preparation of (*E*)-vinylbromides: 4.0 equiv dimethyl phosphite, 4.5 equiv Et_3N, DMF, 70 °C, 12 h; for the (*Z*)-vinylbromides: 0.05 equiv $Pd(PPh_3)_4$, 1.1 equiv Bu_3SnH, benzene, 25 °C, 3 h).[19] Without optimization, these bromides were subjected to the reaction conditions established for preparation of the *N*-aryl derivatives (0.05 equiv $Pd_2(dba)_3$, 0.1 equiv $(Cy)_2P(DMAbp)$, 1.6 equiv Cs_2CO_3, THF, reflux, 3–6 h, 20–43%) to provide **16**–**20** (Scheme 2). Synthesis of the *Z*-olefin *N*-alkenyl CBI derivatives was also possible using the corresponding (*Z*)-vinylbromide. However, facile isomerization to the *E*-olefin occurred during chromatography that resulted in isolation of ⩾9:1 *E*/*Z* mixtures and further studies on the selective preparation of the *Z*-isomers were not pursued or warranted.

2.3. X-ray structures of the *N*-aryl CBI derivatives

Single-crystal X-ray crystal structures were established for **7**–**14** and were conducted on needles obtained by recrystallization from 20% CH_2Cl_2–hexanes for the electron-rich *N*-aryl CBI analogues, or from 10% MeOH–EtOAc for the electron-deficient series.[20] The X-ray data for the series is summarized in Table 1 and Figure 3. Analogous to observations made with the *N*-acyl CBI derivatives, the cyclopropane alignment of the *N*-aryl CBI compounds has the bent orbitals of the longer

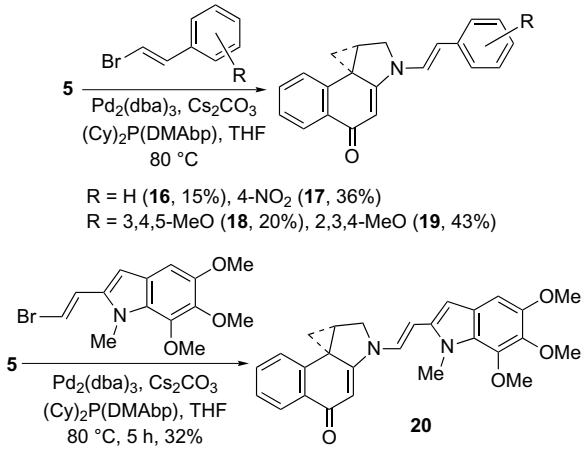

Scheme 2.

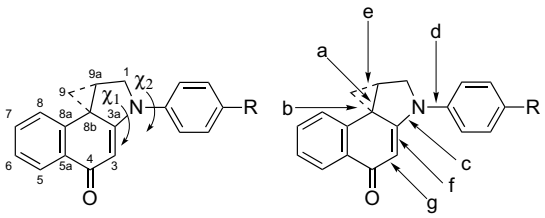

Figure 3. Numbering and bond nomenclature for X-ray structures.

C8b–C9 cyclopropane bond (bond b) aligned with the conjugated cyclohexadienone π-system, whereas those of the alternative and shorter C8b–C9a bond (bond a) are nearly orthogonal consistent with exclusive C9 nucleophilic addition with cleavage of only the weaker (longer) and stereoelectronically aligned C8b–C9 bond (bond b).

More fundamental, diagnostic X-ray bond lengths and the $\chi 1$ and $\chi 2$ dihedral angles could be used to assess the aryl substituent impact (Table 1). Although the correlations are not perfect throughout the entire series and some (e.g., **12**) are clearly influenced by crystal packing forces, there are defined trends that can be observed in the comparison of the structures. Electron-withdrawing *p*-substituents smoothly decrease the d bond length and $\chi 2$ dihedral angle consistent with N2 amine conjugation with the substituent through the aryl ring diminishing the stabilizing vinylogous amide conjugation with the cyclohexadienone π-system. Accordingly, there is an accompanying trend for an increasing c bond length, decreasing f bond length, and increasing $\chi 1$ dihedral angle diagnostic of this loss in vinylogous amide conjugation across the series. Thus, electron-withdrawing substituents would be expected to diminish the vinylogous amide stabilization of the CBI alkylation subunit increasing its reactivity, whereas electron-donating substituents would be expected to enhance this stabilization and diminish the reactivity consistent with the observed trends found in the solvolytic reactivity of the *N*-aryl CBI analogues.

2.4. Reaction regioselectivity

Consistent with the stereoelectronic alignment of the cyclopropane, acid-catalyzed nucleophilic addition to

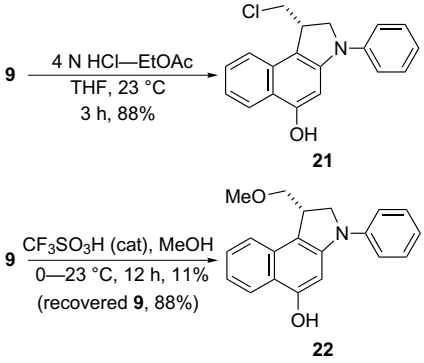

Scheme 3.

9, the parent member of the *N*-aryl CBI series, proceeded exclusively (>20:1) at the least substituted cyclopropane carbon with cleavage of the reactive and aligned C8b–C9 bond (Scheme 3). Notably, this stereoelectronic control overrides any intrinsic preference for ring expansion ring opening with partial positive charge development on the more substituted cyclopropane carbon and may benefit from the preference for S_N2 nucleophilic attack to occur at the least substituted carbon. Thus, treatment of **9** with anhydrous HCl resulted in exclusive formation of **21** in 3 h at 23 °C (88%). Similarly, treatment of **9** with CF_3SO_3H–MeOH (0.02 M CF_3SO_3H, 0–23 °C, 12 h) led to exclusive formation of **22** (11%) derived from MeOH addition to the least substituted cyclopropane carbon along with recovered, unreacted **9** (88%). In both cases, the decreased reactivity of the *N*-aryl derivative relative to typical *N*-acyl CBI derivatives was clear by the need to conduct these reactions at room temperature for prolonged reaction times. This is in contrast to the typical *N*-acyl derivatives where the reactions proceed at much lower temperatures (−78 to 0 °C), with much faster reaction times (<1 h), and proceed to a greater extent (>95% yield).

2.5. Solvolysis reactivity

The derivatives **6**–**15** proved to be remarkably stable displaying readily measurable solvolysis reactivity only at pH 2 (Table 2). This reactivity followed a well-defined correlation with σ_p ($\rho = 0.17$) in which electron-withdrawing substituents enhance and electron-donating

Table 1. Summary of X-ray data for **7**–**14**

	14 R = NO_2	**13** R = CN	**12** R = CO_2CH_3	**11** R = Cl	**10** R = F	**9** R = H	**8** R = Me	**7** R = OMe	*N*-CO_2Me-CBI
X-ray bond lengths									
a	1.521(4)	1.462(7)	1.492(13)	1.519(3)	1.521(3)	1.526(4)	1.518(2)	1.523(3)	1.521(5)
b	1.530(4)	1.558(9)	1.545(12)	1.534(3)	1.535(3)	1.549(4)	1.529(2)	1.538(3)	1.544(5)
c	1.394(3)	1.399(6)	1.490(8)	1.380(3)	1.384(2)	1.395(4)	1.376(2)	1.380(3)	1.390(5)
d	1.389(3)	1.382(6)	1.416(8)	1.397(3)	1.409(3)	1.420(4)	1.410(2)	1.416(3)	1.372(5)
e	1.485(4)	1.428(10)	1.463(12)	1.466(3)	1.474(3)	1.498(5)	1.472(3)	1.489(3)	1.472(5)
f	1.348(3)	1.336(6)	1.341(3)	1.349(3)	1.358(3)	1.362(4)	1.358(2)	1.362(3)	1.396(5)
g	1.444(3)	1.430(7)	1.445(3)	1.427(3)	1.444(3)	1.443(4)	1.438(2)	1.427(3)	1.440(5)
X-ray dihedral angles									
χ_1	19.6°	15.3°	39.2°	14.5°	12.8°	16.2°	11.7°	12.9°	6.9°
χ_2	14.4°	13.8°	13.8°	17.2°	21.6°	22.6°	20.1°	25.5°	4.5°

Table 2. Solvolysis reactivity[a]

Compound	k (s^{-1}, pH2)	$t_{1/2}$ (h)	r
15 (R = 2,4-NO_2)	2.17×10^{-6}	89	0.95
14 (R = NO_2)	1.66×10^{-6}	115	0.99
13 (R = CN)	1.49×10^{-6}	129	0.99
12 (R = CO_2CH_3)	1.38×10^{-6}	138	0.99
11 (R = Cl)	1.24×10^{-6}	155	0.99
10 (R = F)	1.17×10^{-6}	164	0.99
9 (R = H)	1.12×10^{-6}	171	0.99
8 (R = CH_3)	1.03×10^{-6}	187	0.97
7 (R = OCH_3)	0.96×10^{-6}	198	0.97
6 (R = NMe_2)	0.85×10^{-6}	227	0.99

[a] pH = 2: 50% CH_3OH–buffer, buffer is 4:1:20 (v:v:v). 1.0 M citric acid, 0.2 M Na_2HPO_4, and H_2O, respectively.

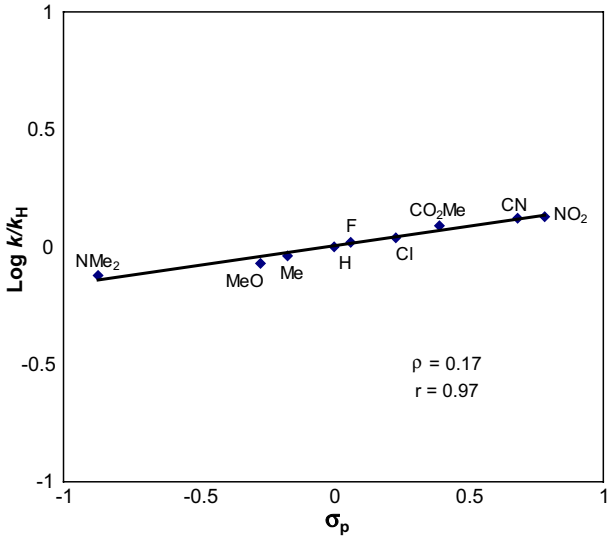

Figure 4. Log k/k_H (solvolysis, pH2) vs σ_p for **6** (NMe_2)–**14** (NO_2).

substituents decrease the solvolysis rate (Fig. 4). Thus, the solvolysis stability correlates with the expected extent of cross-conjugated vinylogous amide stabilization of the cyclohexadienone structure. In turn, this extent of the vinylogous amide conjugation can be observed with the diagnostic bond length and dihedral angle ($\chi1$ and $\chi2$) trends found in the X-rays of **6**–**14**. In contrast to **6**–**15**, the *N*-alkenyl derivatives **16**–**20** did not undergo clean solvolysis. Rather they underwent competitive or predominant vinylogous enamide hydrolysis.

2.6. DNA alkylation properties

A comparison of DNA alkylation efficiency and selectivity of (+)-**9**, (+)-*N*-Boc-CBI, and (+)-duocarmycin SA (**3**) was conducted following protocols previously detailed[21] (Fig. 5). These comparisons revealed that the alkylation selectivity for (+)-**9** was indistinguishable from that of (+)-*N*-Boc-CBI and this is illustrated nicely in Figure 5, where both compounds exclusively alkylate adenine non-selectively (5′-AA or 5′-TA)[22] relative to (+)-duocarmycin SA (e.g., 5′-AAAA).[23] In contrast to (+)-**3** and (+)-CBI-TMI but analogous to (+)-*N*-Boc-CBI, the rate and efficiency of DNA alkylation by (+)-**9** was low. The detectable alkylation for **9** was observed

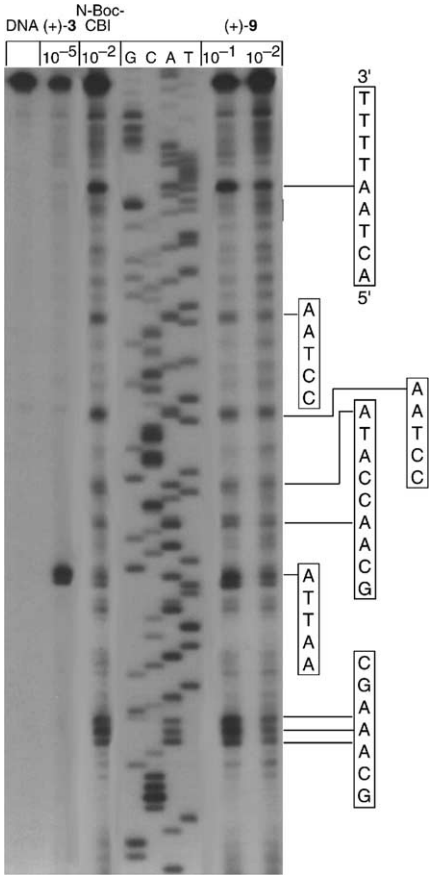

Figure 5. Thermally-induced strand cleavage of w794 DNA (SV40 DNA segment, 144 bp, nucleotide no 138–5238). DNA-agent incubation at 25 °C for (+)-duocarmycin SA (24 h) and 37 °C for *N*-Boc-CBI and (+)-**9** (120 h), removal of unbound agent and 30 min thermolysis (100 °C), followed by denaturing 8% PAGE and autoradiography. Lane 1, control DNA; lane 2, (+)-duocarmycin SA ((+)-**3**, 1×10^{-5} M); lane 3, (+)-*N*-Boc-CBI (1×10^{-2} M); lanes 4–7, Sanger G, C, A, and T reactions; lanes 8–9, (+)-**9** (1×10^{-1} M and 1×10^{-2} M, respectively).

only at high agent concentrations (10^{-2} M vs 10^{-6} M), at increased reaction times (120 h vs 2–24 h), and at elevated reaction temperatures (37 °C vs 5–23 °C). Under the conditions examined, (+)-**9** was slightly slower and less efficient at alkylating DNA than (+)-*N*-Boc-CBI (Fig. 5). Regardless of the origin of the effect, the less effective DNA alkylation by (+)-**9** (ca. 10^4-fold), like that of (+)-*N*-Boc-CBI, correlates well with its less potent cytotoxic activity (roughly 10^4-fold).

2.7. Cytotoxic activity

The biological properties (cytotoxic activity, L1210) of **6**–**14** also exhibited a well-defined trend correlating with their reactivity (Table 3 and Fig. 6). Thus, electron-withdrawing substituents smoothly increase, whereas electron-donating substituents decrease, the cytotoxic activity of the derivatives. The more potent derivatives, **14**, **13**, and **12** (bearing electron-withdrawing substituents) displayed cytotoxic potency (IC_{50} = 40, 140, and 330 nM, respectively) comparable to that of simple *N*-acyl-CBI derivatives (e.g., *N*-Boc-CBI, IC_{50} = 80 nM), that of the naturally occurring alkylation subunits

Table 3. In vitro cytotoxic activity[a]

Compound[b]	IC_{50} (nM)[a]	Compound[c]	IC_{50} (nM)[a]
(+)-*N*-Boc-CBI	80	(−)-*N*-Boc-CBI	900
(+)-**6**	3800	(−)-**6**	>10,000
(−)-**7**	3200	(+)-**7**	18,000
(+)-**8**	1900	(−)-**8**	16,000
(+)-**9**	1100	(−)-**9**	5000
(−)-**10**	670	(+)-**10**	8400
(+)-**11**	530	(−)-**11**	3800
(+)-**12**	330	(−)-**12**	2500
(−)-**13**	140	(+)-**13**	310
(−)-**14**	40	(+)-**14**	1800
(+)-**15**	270	(−)-**15**	500
(+)-**16**	40	(−)-**16**	700
(+)-**17**	10	(−)-**17**	420
(+)-**18**	140	(−)-**18**	680
(−)-**19**	380	(+)-**19**	340
(+)-**20**	17	(−)-**20**	90

[a] L1210 cytotoxic activity, average of 2–7 determinations in triplicate.
[b] Natural enantiomer series.
[c] Unnatural enantiomer series.

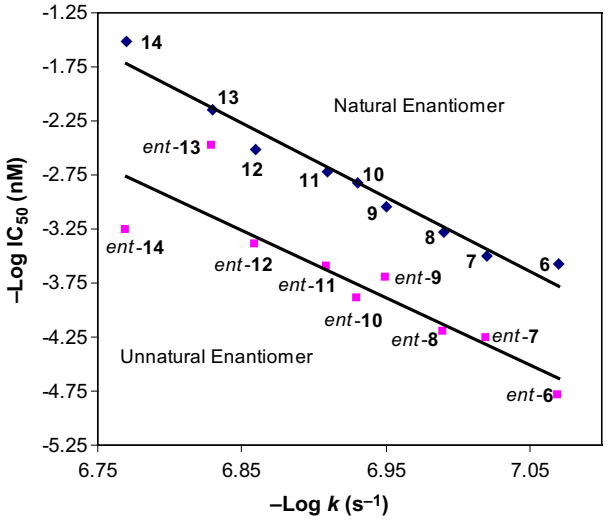

Figure 6. Relationship between reactivity (solvolysis *k*, pH2) and cytotoxic potency (L1210) for **6**–**14**.

(e.g., *N*-Boc-MeCPI, IC_{50} = 300 nM), and in the range of that commonly associated with efficacious antitumor drugs (e.g., mitomycin, IC_{50} = 90 nM). The unnatural enantiomers exhibited an analogous trend, but with approximately a 10-fold reduction in cytotoxic activity compared to the natural enantiomers (Fig. 6).

Each of the *N*-alkenyl CBI derivatives exhibited cytotoxic activity that was comparable to the best of derivatives in the *N*-aryl series and the series exhibited similar trends. Thus, **17** bearing the *p*-nitrophenyl group was 4-fold more potent than the *p*-nitrophenyl-CBI derivative **14**, 4-fold more potent than **16** bearing an unsubstituted phenyl group, and >10-fold more potent than either **18** or **19**. Especially interesting for this series is **20**, which was among the most potent *N*-aryl or *N*-alkenyl CBI derivative examined exhibiting a 20 nM IC_{50} (L1210). This derivative can be viewed as an analogue of CBI-TMI (L1210 IC_{50} = 30 pM) where its linking amide is replaced with the linking alkene. This simple replacement reduces the cytotoxic potency 1000-fold. Nonetheless, it is 100-fold more potent than the corresponding CBI-TMI analogue where the linking amide is replaced by a linking methylene (L1210 IC_{50} = 1.4 μM).[24]

2.8. Establishment of the full parabolic relationship between reactivity and cytotoxic activity

Among the most important of the relationships established with these agents is a direct correlation between chemical stability and biological potency (cytotoxic activity).[5,25] To date, this relationship extends over a 10^6-fold range in both reactivities and activities and covers a wide range of modified alkylation subunits.[5,26] When considering only derivatives that possess sufficient reactivity to alkylate DNA, this has been interpreted to reflect the ability of the chemically more stable derivatives to more effectively reach their biological target (DNA).[5,25] When this correlation between reactivity (−log *k*, pH3) and cytotoxic activity (−log IC_{50}, L1210) for **6**–**14** is plotted with the data for the more reactive *N*-acyl alkylation subunit derivatives, it established a well-defined parabolic relationship between reactivity and biological potency (Figs. 7 and 8). These plots, in which the unnatural enantiomers (Fig. 8) are 5- to 10-fold less potent than the natural enantiomers (Fig. 7), incorporate not only the *N*-aryl derivatives **6**–**15**, but all *N*-Boc derivatives of the alkylation subunits that we have examined to date (Fig. 9).[27] The parabolic relationship defined by these correlations establishes that the compounds should possess sufficient stability to reach their biological target (DNA), yet maintain sufficient reactivity to alkylate DNA upon reaching the biological target. Just as importantly, it defines the optimal balance of stability/reactivity that may be used for the future design of related analogues.

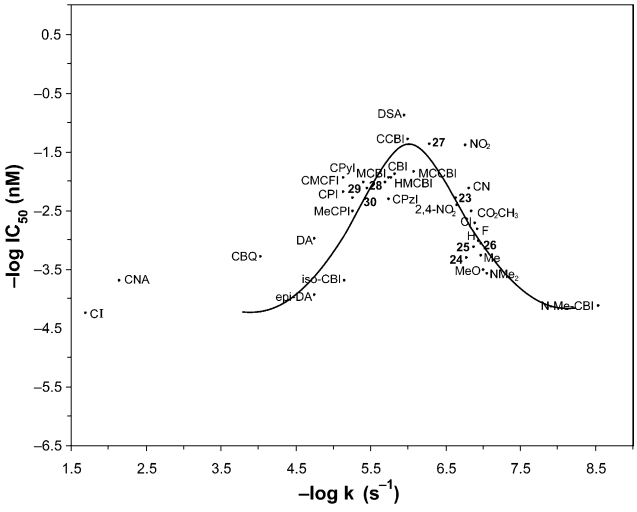

Figure 7. Relationship between reactivity (solvolysis *k*, pH3) and cytotoxic potency (L1210), natural enantiomers. The notations NMe_2, OMe, Me, H, F, Cl, CO_2Me, CN, NO_2, and 2,4-NO_2 refer to **6**–**15**, respectively (Scheme 1), and structures of the remaining compounds are provided in Figure 9.

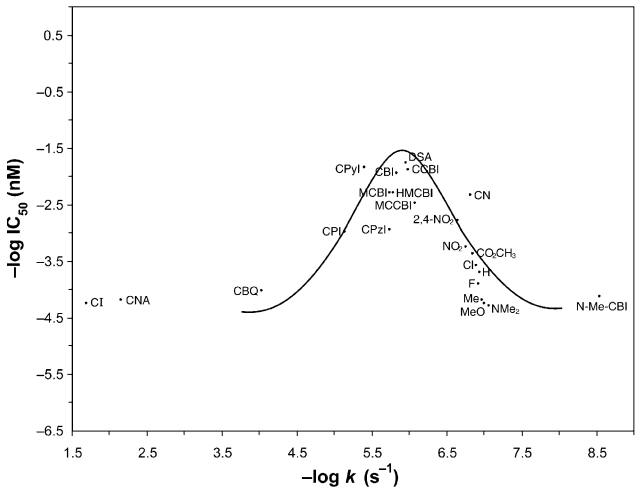

Figure 8. Relationship between reactivity (solvolysis k, pH 3) and cytotoxic potency (L1210), unnatural enantiomers. The notations NMe_2, OMe, Me, H, F, Cl, CO_2Me, CN, NO_2, and 2,4-NO_2 refer to **6**–**15**, respectively (Scheme 1), and structures of the remaining compounds are provided in Figure 9.

Notably, the duocarmycin SA alkylation subunit (DSA) also found in yatakemycin lies at the optimal stability/reactivity position on this plot, whereas the CC-1065 (MeCPI) and duocarmycin A (DA) alkylation subunits lie progressively and significantly to the left. In addition to indicating that duocarmycin SA and yatakemycin may be the most exciting of the natural products to pursue, it is tempting to suggest that duocarmycin A and CC-1065 may represent intermediate steps in Nature's evolution of optimal DNA alkylating compounds (duocarmycin SA and yatakemycin).

The variations that appear in this correlation may be attributed not only to the inherent error in the cytotoxic assay with data that has been collected intermittently over 15 years, but also to structural differences in the derivatives that impact features beyond reactivity (e.g., cell penetration and distribution, DNA binding affinity). Even without accounting for such variables, the adherence to the parabolic relationship is remarkable, consistent with a correlation of fundamental importance.

3. Conclusions

The preparation of a novel series of *N*-aryl and *N*-alkenyl CBI derivatives is detailed in which an aryl substituent could be used to predictably modulate the reactivity of the resulting alkylation subunit analogue of a series of natural products that now include **1**–**4**. The *N*-aryl derivatives were found to be exceptionally stable and to exhibit well-defined relationships between structure, reactivity, and cytotoxic potency. Not only do the derivatives constitute novel and active CBI derivatives, but when combined with the results of an extensive series of *N*-acyl alkylation subunit analogues and derivatives assembled over the past 15 years, the studies define a fundamental parabolic relationship between reactivity and cytotoxic potency.

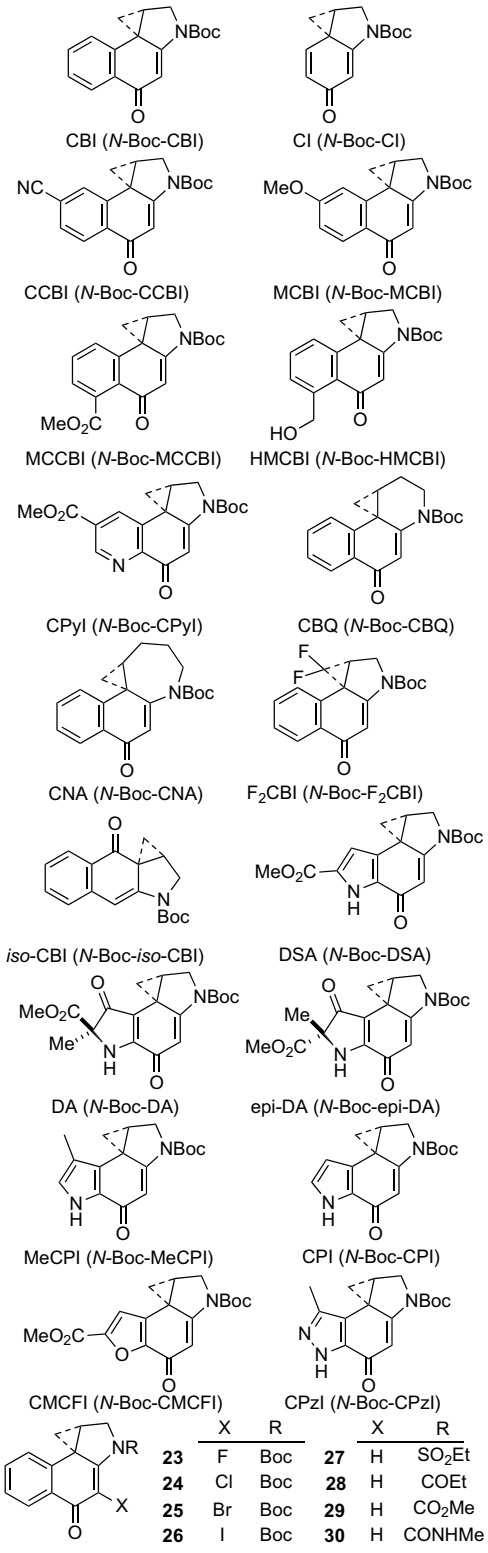

Figure 9. Structures of compounds for Figure 7.

4. Experimental

4.1. *N*-(4-Dimethylaminophenyl)-1,2,9,9a-tetrahydropropa[*c*]benz[*e*]indol-4-one (6)

A mixture of CBI (2.5 mg, 12.6 μmol), tri-*p*-dimethylaminophenylbismuth (14.4 mg, 25.2 μmol), and

$Cu(OAc)_2$ (3.4 mg, 18.9 μmol) in CH_2Cl_2 (130 μL) was treated with Et_3N (2.6 μL, 18.9 μmol) and stirred under Ar at 25 °C for 36 h. The reaction mixture was diluted with EtOAc (30 mL), washed with saturated aqueous NH_4Cl (1 × 10 mL), dried (Na_2SO_4), and concentrated. PTLC (SiO_2, 20 × 20 cm, EtOAc) afforded **6** (2.5 mg, 63%) as a yellow solid: mp 60–62 °C; R_f = 0.34 (EtOAc); ^{1}H NMR (acetone-d_6, 500 MHz) δ 8.06 (d, J = 8.1 Hz, 1H), 7.46 (t, J = 7.4 Hz, 1H), 7.34 (t, J = 7.4 Hz, 1H), 7.19 (d, J = 9.2 Hz, 2H), 7.07 (d, J = 7.7 Hz, 1H), 6.81 (d, J = 8.8 Hz, 2H), 5.57 (s, 1H), 4.38 (dd, J = 10.3, 5.2 Hz, 1H), 3.79 (d, J = 10.3 Hz, 1H), 3.05 (m, 1H), 2.96 (s, 6H), 1.65 (dd, J = 7.7, 4.0 Hz, 1H), 1.52 (t, J = 4.4 Hz, 1H); ^{13}C NMR ($CDCl_3$, 100 MHz) δ 184.5, 166.2, 148.8, 139.5, 133.8, 130.7, 129.0, 126.6, 126.2, 123.8 (2C), 120.6, 112.9 (2C), 97.2, 57.3, 40.7 (2C), 38.3, 29.7, 22.8; IR (film) ν_{max} 2924, 1602, 1593, 1519, 1444, 1352, 1270 cm^{-1}; HRMALDI-FTMS (DHB) m/z 317.1654 ($M+H^+$, $C_{21}H_{20}N_2O$ requires 317.1648). Natural-**6**: $[\alpha]_D^{23}$ +181 (*c* 0.04, acetone); *ent*-**6**: $[\alpha]_D^{23}$ −187 (*c* 0.035, acetone).

4.2. *N*-(4-Methoxyphenyl)-1,2,9,9a-tetrahydropropa[*c*]-benz[*e*]indol-4-one (7)

A mixture of CBI (4.7 mg, 24 μmol), tri-*p*-methoxyphenylbismuth (25.3 mg, 48 μmol), and $Cu(OAc)_2$ (6.5 mg, 36 μmol) in CH_2Cl_2 (60 μL) was treated with Et_3N (5.0 μL, 36 μmol) and stirred under Ar at 25 °C for 24 h. The reaction mixture was diluted with EtOAc (30 mL), washed with saturated aqueous NH_4Cl (1 × 10 mL), dried (Na_2SO_4), and concentrated. PTLC (SiO_2, 10 × 20 cm, 20% EtOAc–CH_2Cl_2) afforded 3-(4-methoxyphenyl)-1,2,9,9a-tetrahydropropa[*c*]benz[*e*]indol-4-one (1.1 mg, 15%) as an off-white film and **7** (4.0 mg, 53%) as an off-white solid. For **7**: mp 159–160 °C; R_f = 0.17 (50% EtOAc–hexanes); ^{1}H NMR (acetone-d_6, 400 MHz) δ 8.07 (d, J = 7.8 Hz, 1H), 7.46 (t, J = 7.6 Hz, 1H), 7.35 (d, J = 8.6 Hz, 1H), 7.30 (d, J = 6.8 Hz, 2H), 7.07 (d, J = 7.6 Hz, 1H), 7.00 (d, J = 6.7 Hz, 2H), 5.63 (s, 1H), 4.42 (dd, J = 10.1, 5.2 Hz, 1H), 3.82 (s, 3H), 3.81 (d, J = 10.1 Hz, 1H), 3.07 (m, 1H), 1.66 (dd, J = 7.8, 4.0 Hz, 1H), 1.55 (t, J = 4.4 Hz, 1H); ^{13}C NMR (acetone-d_6, 150 MHz) δ 183.4, 167.4, 166.2, 164.0, 158.4, 141.0, 134.1, 131.5, 126.6 (2C), 125.1, 122.4, 115.4 (2C), 97.2, 57.7, 55.8, 34.3, 29.7, 23.8; IR (film) ν_{max} 2919, 2849, 1596 cm^{-1}; HRMALDI-FTMS (DHB) m/z 304.1335 ($M+H^+$, $C_{20}H_{17}NO_2$ requires 304.1332). Natural-**7**: $[\alpha]_D^{23}$ −80 (*c* 0.02, THF); *ent*-**7**: $[\alpha]_D^{23}$ +90 (*c* 0.02, THF). A sample of (±)-**7** for X-ray analysis was obtained by recrystallization from 20% CH_2Cl_2–hexanes providing colorless needles (CCDC 216387).

For 3-(4-methoxyphenyl)-1,2,9,9a-tetrahydropropa[*c*]-benz[*e*]indol-4-one: ^{1}H NMR (acetone-d_6, 400 MHz) δ 8.13 (d, J = 7.8 Hz, 1H), 7.44 (t, J = 7.4 Hz, 1H), 7.35 (t, J = 7.8 Hz, 1H), 7.26 (d, J = 8.8 Hz, 2H), 7.04 (d, J = 7.6 Hz, 1H), 6.88 (d, J = 8.8 Hz, 2H), 6.31 (br s, 1H), 3.77 (s, 3H), 3.76 (m, 1H), 3.65 (d, J = 10.6 Hz, 1H), 3.06 (m, 1H), 1.65 (dd, J = 7.9, 3.7 Hz, 1H), 1.46 (t, J = 4.7 Hz, 1H); IR (film) ν_{max} 3378, 2919, 1596, 1531 cm^{-1}; HRMALDI-FTMS (DHB) m/z 304.1327 ($M+H^+$, $C_{20}H_{17}NO_2$ requires 304.1332). Natural enantiomer: $[\alpha]_D^{23}$ −19 (*c* 0.16, THF); unnatural enantiomer: $[\alpha]_D^{23}$ +22 (*c* 0.20, THF).

4.3. *N*-(4-Methylphenyl)-1,2,9,9a-tetrahydropropa[*c*]-benz[*e*]indol-4-one (8)

A mixture of CBI (4.9 mg, 24 μmol), tri-*p*-methylphenylbismuth (18.0 mg, 37 μmol), and $Cu(OAc)_2$ (6.8 mg, 37 μmol) in CH_2Cl_2 (100 μL) was treated with Et_3N (5.2 μL, 37 μmol) and stirred under Ar at 25 °C for 24 h. The reaction mixture was diluted with EtOAc (30 mL), washed with saturated aqueous NH_4Cl (1 × 10 mL), dried (Na_2SO_4), and concentrated. PTLC (SiO_2, 10 × 20 cm, 20% EtOAc–CH_2Cl_2) afforded 3-(4-methylphenyl)-1,2,9,9a-tetrahydropropa[*c*]benz[*e*]indol-4-one (0.9 mg, 13%) as an off-white film and **8** (2.8 mg, 39%) as an off-white solid. For **8**: mp 154–155 °C; R_f = 0.33 (50% EtOAc–hexanes); ^{1}H NMR (acetone-d_6, 400 MHz) δ 8.07 (d, J = 7.8 Hz, 1H), 7.47 (app t, J = 7.5 Hz, 1H), 7.34 (app t, J = 7.4 Hz, 1H), 7.25 (br s, 4H), 7.08 (d, J = 7.8 Hz, 1H), 5.81 (s, 1H), 4.47 (dd, J = 10.1, 5.1 Hz, 1H), 3.82 (d, J = 10.2 Hz, 1H), 3.07 (m, 1H), 2.33 (s, 3H), 1.67 (dd, J = 7.8, 4.0 Hz, 1H), 1.54 (t, J = 4.6 Hz, 1H); ^{13}C NMR (acetone-d_6, 150 MHz) δ 183.6, 165.4, 164.1, 141.1, 138.9, 135.5, 134.6, 131.7 (2C), 130.7, 129.4, 126.8, 122.8 (2C), 98.0, 57.2, 34.3, 26.4, 23.7, 20.8; IR (film) ν_{max} 2919, 1596, 1555 cm^{-1}; HRMALDI-FTMS (DHB) m/z 288.1377 ($M+H^+$, $C_{20}H_{17}NO$ requires 288.1383). Natural-**8**: $[\alpha]_D^{23}$ +120 (*c* 0.06, THF); *ent*-**8**: $[\alpha]_D^{23}$ −125 (*c* 0.12, THF). A sample of (±)-**8** for X-ray analysis was obtained by recrystallization from 20% CH_2Cl_2–hexanes providing beige plates (CCDC 216389).

For 3-(4-methylphenyl)-1,2,9,9a-tetrahydropropa[*c*]benz-[*e*]indol-4-one: ^{1}H NMR (acetone-d_6, 500 MHz) δ 8.13 (d, J = 7.7 Hz, 1H), 7.44 (d, J = 7.7 Hz, 1H), 7.34 (t, J = 7.7 Hz, 1H), 7.23 (d, J = 8.1 Hz, 2H), 7.12 (d, J = 7.7 Hz, 2H), 7.04 (d, J = 7.0 Hz, 1H), 6.33 (br s, 1H), 3.80 (ddd, J = 10.6, 5.1, 1.5 Hz, 1H), 3.65 (d, J = 10.7 Hz, 1H), 3.06 (m, 1H), 2.31 (s, 3H), 1.65 (dd, J = 8.1, 4.0 Hz, 1H), 1.46 (t, J = 4.4 Hz, 1H); IR (film) ν_{max} 3389, 2908, 1596 cm^{-1}; HRMALDI-FTMS (DHB) m/z 288.1377 ($M+H^+$, $C_{20}H_{17}NO$ requires 288.1383). Natural enantiomer: $[\alpha]_D^{23}$ −14 (*c* 0.10, THF); unnatural enantiomer: $[\alpha]_D^{23}$ +18 (*c* 0.18, THF).

4.4. *N*-Phenyl-1,2,9,9a-tetrahydropropa[*c*]benz[*e*]indol-4-one (9)

A mixture of CBI (4.7 mg, 24 μmol), triphenylbismuth (12.6 mg, 29 μmol), and $Cu(OAc)_2$ (4.8 mg, 26 μmol) in CH_2Cl_2 (60 μL) was treated with Et_3N (3.3 L, 24 μmol) and stirred under Ar at 25 °C for 18 h. The reaction mixture was diluted with EtOAc (30 mL), washed with saturated aqueous NH_4Cl (1 × 10 mL), dried (Na_2SO_4), and concentrated. PTLC (SiO_2, 10 × 20 cm, 20% EtOAc–CH_2Cl_2) afforded 3-phenyl-1,2,9,9a-tetrahydropropa[*c*]benz[*e*]indol-4-one (0.5 mg, 8%) as an off-white film and **9** (3.3 mg, 51%) as an off-white solid. For **9**: mp 145–146 °C (dec); R_f = 0.50 (EtOAc); ^{1}H NMR

(acetone-d_6, 400 MHz) δ 8.06 (d, J = 7.9 Hz, 1H), 7.45 (m, 3H), 7.37 (m, 3H), 7.21 (app t, J = 7.3 Hz, 1H), 7.09 (d, J = 7.6 Hz, 1H), 5.90 (s, 1H), 4.51 (dd, J = 10.1, 5.2 Hz, 1H), 3.85 (d, J = 10.1 Hz, 1H), 3.08 (m, 1H), 1.70 (dd, J = 7.8, 4.1 Hz, 1H), 1.57 (t, J = 4.5 Hz, 1H); ^{13}C NMR ($CDCl_3$, 150 MHz) δ 184.5, 164.1, 162.9, 139.9, 139.5, 130.9, 129.2 (2C), 126.4, 126.1, 124.8, 121.1 (2C), 120.6, 98.7, 56.0, 33.5, 29.0, 22.4; IR (film) ν_{max} 2933, 2882, 1615, 1589 cm^{-1}; HRMALDI-FTMS (DHB) m/z 274.1220 ($M+H^+$, $C_{19}H_{15}NO$ requires 274.1226). Natural-**9**: $[\alpha]_D^{23}$ + 210 (c 0.15, THF); *ent*-**9**: $[\alpha]_D^{23}$ − 200 (c 0.02, THF). A sample of (±)-**9** for X-ray analysis was obtained by recrystallization from 20% CH_2Cl_2–hexanes providing colorless needles (CCDC 216392).

For 3-phenyl-1,2,9,9a-tetrahydropropa[c]benz[e]indol-4-one: ^{1}H NMR (acetone-d_6, 400 MHz) δ 8.13 (d, J = 7.8 Hz, 1H), 7.44 (t, J = 7.5 Hz, 1H), 7.34 (m, 5H), 7.18 (app t, J = 8.5 Hz, 1H), 7.05 (d, J = 7.2 Hz, 1H), 6.39 (br s, 1H), 3.80 (dd, J = 13.3, 5.1 Hz, 1H), 3.65 (d, J = 13.4 Hz, 1H), 3.07 (m, 1H), 1.65 (dd, J = 7.9, 3.8 Hz, 1H), 1.47 (t, J = 4.5 Hz, 1H); IR (film) ν_{max} 3313, 2923, 1580, 1539 cm^{-1}; HRMALDI-FTMS (DHB) m/z 274.1214 ($C_{19}H_{15}NO + H^+$ requires 274.1226). Natural enantiomer: $[\alpha]_D^{23}$ − 34 (c 0.10, THF); unnatural enantiomer: $[\alpha]_D^{23}$ + 38 (c 0.10, THF).

4.5. *N*-(4-Fluorophenyl)-1,2,9,9a-tetrahydropropa[*c*]-benz[*e*]indol-4-one (10)

A mixture of CBI (2.5 mg, 12.6 μmol), tri-*p*-fluorophenylbismuth (12.6 mg, 25.2 μmol), and $Cu(OAc)_2$ (3.4 mg, 18.9 μmol) in CH_2Cl_2 (130 μL) was treated with Et_3N (2.6 μL, 18.9 μmol) and stirred under Ar at 25 °C for 36 h. The reaction mixture was diluted with EtOAc (30 mL), washed with saturated aqueous NH_4Cl (1 × 10 mL), dried (Na_2SO_4), and concentrated. PTLC (SiO_2, 20 × 20 cm, 40% EtOAc–hexanes) afforded **10** (2.1 mg, 57%) as a yellow solid: mp 154–156 °C; R_f = 0.52 (EtOAc); ^{1}H NMR ($CDCl_3$, 500 MHz) δ 8.23 (d, J = 6.6 Hz, 1H), 7.47 (t, J = 6.2 Hz, 1H), 7.39 (t, J = 6.6 Hz, 1H), 7.23 (m, 2H), 7.10 (m, 2H), 6.88 (d, J = 6.6 Hz, 1H), 6.01 (s, 1H), 4.35 (dd, J = 8.0, 4.1 Hz, 1H), 3.79 (d, J = 8.0 Hz, 1H), 2.86 (m, 1H), 1.68 (dd, J = 6.2, 2.5 Hz, 1H), 1.53 (t, J = 2.5 Hz, 1H); ^{13}C NMR ($CDCl_3$, 125 MHz) δ 185.1, 165.2, 161.3, 140.0, 133.9, 131.5, 127.1, 126.8, 124.0 (2C), 121.2, 116.9, 116.7 (2C), 98.8, 57.1, 34.1, 29.7, 23.3; IR (film) ν_{max} 3063, 2961, 1622, 1592, 1558, 1230, 1031 cm^{-1}; HRMALDI-FTMS (DHB) m/z 292.1129 ($M+H^+$, $C_{19}H_{14}FNO$ requires 292.1132). Natural-**10**: $[\alpha]_D^{23}$ − 155 (c 1.0, $CHCl_3$); *ent*-**10**: $[\alpha]_D^{23}$ + 151 (c 1.0, $CHCl_3$). A sample of (±)-**10** for X-ray analysis was obtained by recrystallization from 20% CH_2Cl_2–hexanes providing colorless needles (CCDC 216388).

4.6. *N*-(4-Chlorophenyl)-1,2,9,9a-tetrahydropropa[*c*]-benz[*e*]indol-4-one (11)

A mixture of CBI (2.5 mg, 12.7 μmol), tri-*p*-chlorophenylbismuth (13.7 mg, 25.3 μmol), and $Cu(OAc)_2$ (3.5 mg, 19.1 μmol) in CH_2Cl_2 (130 μL) was treated with Et_3N (2.7 μL, 19.1 μmol) and stirred under Ar at 25 °C for 36 h. The reaction mixture was diluted with EtOAc (1 mL), washed with saturated aqueous NH_4Cl (1 × 10 mL), dried (Na_2SO_4), and concentrated. PTLC (SiO_2, 20 × 20 cm, 40% EtOAc–hexanes) afforded **11** (2.5 mg, 64%) as a yellow solid: mp 194–196 °C; R_f = 0.58 (EtOAc); ^{1}H NMR ($CDCl_3$, 500 MHz) δ 8.31 (d, J = 6.6 Hz, 1H), 7.53 (t, J = 7.7 Hz, 1H), 7.51 (t, J = 7.7 Hz, 1H), 7.41 (m, 2H), 7.34 (m, 2H), 7.25 (d, J = 7.7 Hz, 1H), 6.21 (s, 1H), 4.45 (dd, J = 10.3, 5.2 Hz, 1H), 3.87 (d, J = 10.3 Hz, 1H), 2.92 (m, 1H), 1.73 (dd, J = 10.3, 4.2 Hz, 1H), 1.57 (t, J = 4.2 Hz, 1H); ^{13}C NMR ($CDCl_3$, 125 MHz) δ 185.2, 161.3, 140.0, 139.2, 134.1, 133.7, 131.7, 130.0 (2C), 127.1, 126.8, 122.8 (2C), 121.3, 99.7, 56.6, 34.1, 29.6, 23.1; IR (film) ν_{max} 3285, 3060, 2960, 1588, 1554, 1493, 1272 cm^{-1}; HRMALDI-FTMS (DHB) m/z 308.0834 ($M+H^+$, $C_{19}H_{14}ClNO$ requires 308.0837). Natural-**11**: $[\alpha]_D^{23}$ + 125 (c 1.0, $CHCl_3$); *ent*-**11**: $[\alpha]_D^{23}$ − 128 (c 1.0, $CHCl_3$). A sample of (±)-**11** for X-ray analysis was obtained by recrystallization from 20% CH_2Cl_2–hexanes providing colorless plates (CCDC 216391).

4.7. *N*-(4-Methoxycarbonylphenyl)-1,2,9,9a-tetrahydropropa[*c*]benz[*e*]indol-4-one (12)

A mixture of CBI (2.5 mg, 12.6 μmol), methyl-4-chlorobenzoate (3.2 mg, 18.9 μmol), Cs_2CO_3 (6.6 mg, 20.2 μmol), $Pd_2(dba)_3$ (0.6 mg, 0.63 μmol), and 2-dicyclohexylphosphino-2′-(*N*,*N*-dimethylamino)-biphenyl (0.5 mg, 1.26 μmol) in THF (130 μL) under Ar was warmed at reflux for 3 h. The reaction mixture was diluted with EtOAc (30 mL), washed with saturated aqueous NH_4Cl (1 × 10 mL), dried (Na_2SO_4), and concentrated. PTLC (SiO_2, 20 × 20 cm, 40% EtOAc–hexanes) afforded **12** (2.7 mg, 65%) as a yellow solid: mp 191–193 °C (dec); R_f = 0.38 (EtOAc); ^{1}H NMR ($CDCl_3$, 500 MHz) δ 8.24 (d, J = 7.6 Hz, 1H), 8.05 (d, J = 9.2 Hz, 2H), 7.50 (t, J = 6.6 Hz, 1H), 7.41 (t, J = 7.4 Hz, 1H), 7.30 (d, J = 8.8 Hz, 2H), 6.91 (d, J = 7.7 Hz, 1H), 6.40 (s, 1H), 4.44 (dd, J = 9.9, 5.1 Hz, 1H), 3.93 (s, 3H), 3.84 (d, J = 9.9 Hz, 1H), 2.86 (m, 1H), 1.72 (dd, J = 7.7, 4.4 Hz, 1H), 1.54 (t, J = 4.8 Hz, 1H); ^{13}C NMR ($CDCl_3$, 125 MHz) δ 185.4, 163.1, 144.9, 140.2, 133.9, 131.9 (2C), 131.5, 127.2, 126.9, 125.9, 121.4, 119.8 (2C), 106.3, 101.6, 56.1, 52.6, 34.0, 29.3, 23.1; IR (film) ν_{max} 2951, 1714, 1621, 1593, 1556, 1512, 1274, 1180 cm^{-1}; HRMALDI-FTMS (DHB) m/z 332.1274 ($M+H^+$, $C_{21}H_{17}NO_3$ requires 332.1281). Natural-**12**: $[\alpha]_D^{23}$ + 37 (c 1.0, $CHCl_3$); *ent*-**12**: $[\alpha]_D^{23}$ − 35 (c 1.0, $CHCl_3$). A sample of (±)-**12** for X-ray analysis was obtained by recrystallization from 10% MeOH–EtOAc providing colorless plates (CCDC 216385).

4.8. *N*-(4-Cyanophenyl)-1,2,9,9a-tetrahydropropa[*c*]-benz[*e*]indol-4-one (13)

A mixture of CBI (3.9 mg, 20 μmol), 4-cyano-1-chlorobenzene (4.1 mg, 30 μmol), Cs_2CO_3 (10.3 mg, 32 μmol), $Pd_2(dba)_3$ (0.9 mg, 1 μmol), and 2-dicyclohexylphosphino-2′-(*N*,*N*-dimethylamino)biphenyl (0.8 mg, 2 μmol) in THF (200 μL) under Ar was warmed at reflux for 8 h. The reaction mixture was diluted with EtOAc

(30 mL), washed with saturated aqueous NH_4Cl (1×10 mL), dried (Na_2SO_4), and concentrated. Flash chromatography (SiO_2, 1×10 cm, 2% MeOH–CH_2Cl_2) afforded **13** (3.1 mg, 53%) as a white solid: mp 213–215 °C (dec); $R_f = 0.45$ (EtOAc); ^{1}H NMR (acetone-d_6, 500 MHz) 8.08 (d, $J = 8.1$ Hz, 1H), 7.81 (d, $J = 8.8$ Hz, 2H), 7.54 (m, 1H), 7.51 (d, $J = 8.8$ Hz, 2H), 7.38 (app t, $J = 7.8$ Hz, 1H), 7.13 (d, $J = 7.7$ Hz, 1H), 6.20 (s, 1H), 4.56 (dd, $J = 9.9$, 5.2 Hz, 1H), 3.93 (d, $J = 9.9$ Hz, 1H), 3.13 (m, 1H), 1.76 (dd, $J = 7.7$, 4.1 Hz, 1H), 1.64 (t, $J = 4.4$ Hz, 1H); ^{13}C NMR (acetone-d_6, 125 MHz) δ 184.4, 163.3, 145.9, 141.4, 134.4 (2C), 134.1, 132.4, 127.0, 126.9, 122.9, 121.4 (2C), 119.4, 107.1, 101.6, 56.4, 34.2, 29.2, 24.0; IR (film) ν_{max} 2913, 2841, 2215, 1621, 1590 cm^{-1}; HRMALDI-FTMS (DHB) *m/z* 299.1185 (M+H$^+$, $C_{20}H_{14}N_2O$ requires 299.1179). Natural-**13**: $[\alpha]_D^{23}$ −300 (*c* 0.02, THF); *ent*-**13**: $[\alpha]_D^{23}$ +280 (*c* 0.02, THF). A sample of (−)-**13** for X-ray analysis was obtained by recrystallization from 10% MeOH–EtOAc providing colorless plates (CCDC 216386).

4.9. *N*-(4-Nitrophenyl)-1,2,9,9a-tetrahydropropa[*c*]-benz[*e*]indol-4-one (14)

A mixture of CBI (3.9 mg, 20 μmol), 4-nitro-1-chlorobenzene (4.7 mg, 30 μmol), Cs_2CO_3 (10.3 mg, 32 μmol), $Pd_2(dba)_3$ (0.9 mg, 1 μmol), and 2-dicyclohexylphosphino-2′-(*N*,*N*-dimethylamino)biphenyl (0.8 mg, 2 μmol) in THF (200 μL) under Ar was warmed at reflux for 3 h. The reaction mixture was diluted with EtOAc (30 mL), washed with saturated aqueous NH_4Cl (1×10 mL), dried (Na_2SO_4), and concentrated. PTLC (SiO_2, 10×20 cm, 50% EtOAc–hexanes) afforded **14** (6.0 mg, 96%) as a tan solid: mp 159–160 °C (dec); $R_f = 0.49$ (EtOAc); ^{1}H NMR (acetone-d_6, 400 MHz) δ 8.31 (d, $J = 9.0$ Hz, 2H), 8.08 (d, $J = 7.8$ Hz, 1H), 7.55 (d, $J = 9.1$ Hz, 2H), 7.54 (app t, $J = 6.8$ Hz, 1H), 7.40 (app t, $J = 7.5$ Hz, 1H), 7.15 (d, $J = 7.8$ Hz, 1H), 6.29 (s, 1H), 4.60 (dd, $J = 10.0$, 5.1 Hz, 1H), 4.00 (d, $J = 10.0$ Hz, 1H), 3.16 (m, 1H), 1.79 (dd, $J = 7.8$, 4.2 Hz, 1H), 1.67 (app t, $J = 4.7$ Hz, 1H); ^{13}C NMR ($CDCl_3$, 150 MHz) δ 184.2, 163.1, 147.4, 139.6, 131.8, 126.9, 126.7, 125.5 (2C), 121.1, 119.1 (2C), 111.7, 102.7, 98.8, 55.6, 34.3, 28.6, 22.8; IR (film) ν_{max} 2923, 2841, 1626, 1585, 1497, 1292 cm^{-1}; HRMALDI-FTMS (DHB) *m/z* 319.1070 (M+H$^+$, $C_{19}H_{14}N_2O_3$ requires 319.1077). Natural-**14**: $[\alpha]_D^{23}$ −80 (*c* 0.10, THF); *ent*-**14**: $[\alpha]_D^{23}$ +80 (*c* 0.10, THF). A sample of (+)-**14** for X-ray analysis was obtained by recrystallization from 10% MeOH–EtOAc providing colorless plates (CCDC 216390).

4.10. *N*-(2,4-Dinitrophenyl)-1,2,9,9a-tetrahydropropa[*c*]-benz[*e*]indol-4-one (15)

A mixture of CBI (3.1 mg, 16 μmol), 2,4-dinitro-1-chlorobenzene (4.8 mg, 24 μmol), Cs_2CO_3 (8.2 mg, 25 μmol), $Pd_2(dba)_3$ (0.7 mg, 0.8 μmol), and 2-dicyclohexylphosphino-2′-(*N*,*N*-dimethylamino)biphenyl (0.6 mg, 1.5 μmol) in THF (160 μL) under Ar was warmed at reflux for 3 h. The reaction mixture was diluted with EtOAc (30 mL), washed with saturated aqueous NH_4Cl (1×10 mL), dried (Na_2SO_4), and concentrated. PTLC (SiO_2, 10×20 cm, 50% EtOAc–hexanes) afforded **15** (3.1 mg, 54%) as an orange solid: mp 162–163 °C (dec); $R_f = 0.20$ (50% EtOAc–hexanes); ^{1}H NMR ($CDCl_3$, 500 MHz) δ 8.80 (d, $J = 2.6$ Hz, 1H), 8.61 (dd, $J = 9.1$, 2.6 Hz, 1H), 8.05 (d, $J = 6.9$ Hz, 1H), 7.93 (d, $J = 9.1$ Hz, 1H), 7.54 (app t, $J = 9.0$ Hz, 1H), 7.39 (m, 1H), 7.16 (d, $J = 7.8$ Hz, 1H), 5.56 (s, 1H), 4.74 (dd, $J = 9.7$, 5.0 Hz, 1H), 4.09 (d, $J = 9.7$ Hz, 1H), 3.21 (m, 1H), 1.87 (dd, $J = 7.6$, 3.5, 1H), 1.82 (t, $J = 5.0$ Hz, 1H); ^{13}C NMR ($CDCl_3$, 150 MHz) δ 184.2, 163.1, 162.1, 143.4, 139.2, 138.9, 132.7, 131.9, 128.6, 126.8, 126.6, 124.8, 122.3, 121.1, 101.8, 56.5, 32.9, 28.2, 24.0; IR (film) ν_{max} 2943, 1619, 1590 cm^{-1}; HRMALDI-FTMS (DHB) *m/z* 364.0940 (M+H$^+$, $C_{19}H_{13}N_3O_5$ requires 364.0928). Natural-**15**: $[\alpha]_D^{23}$ +411 (*c* 0.22, THF); *ent*-**15**: $[\alpha]_D^{23}$ −415 (*c* 0.22, THF).

4.11. *N*-(*E*-2-(4-Phenyl)-1-ethenyl)-1,2,9,9a-tetrahydropropa[*c*]benz[*e*]indol-4-one (16)

A mixture of CBI (12.2 mg, 62 μmol), β-bromostyrene (*E*/*Z* mixture, 12 μL, 93 μmol), Cs_2CO_3 (32.2 mg, 99 μmol), $Pd_2(dba)_3$ (2.8 mg, 3 μmol), and 2-dicyclohexylphosphino-2′-(*N*,*N*-dimethylamino)biphenyl (2.4 mg, 6 μmol) in THF (620 μL) under Ar was warmed at reflux for 4 h. The reaction mixture was diluted with EtOAc (30 mL), washed with saturated aqueous NH_4Cl (1×10 mL), dried (Na_2SO_4), and concentrated. PTLC (SiO_2, 20×20 cm, 50% EtOAc–hexanes) afforded **16** (2.7 mg, 15%) as a yellow solid: $R_f = 0.62$ (50% EtOAc–hexanes); ^{1}H NMR (acetone-d_6, 500 MHz) δ 8.08 (d, $J = 6.3$ Hz, 1H), 7.55 (d, $J = 14.3$ Hz, 1H), 7.49 (m, 3H), 7.36 (t, $J = 6.6$ Hz, 1H), 7.28 (app t, $J = 7.4$ Hz, 2H), 7.14 (t, $J = 7.3$ Hz, 1H), 7.09 (d, $J = 7.3$ Hz, 1H), 6.10 (d, $J = 14.3$ Hz, 1H), 6.06 (s, 1H), 4.10 (dd, $J = 10.6$, 5.5 Hz, 1H), 3.96 (d, $J = 10.7$ Hz, 1H), 3.16 (m, 1H), 1.66 (dd, $J = 7.7$, 4.0 Hz, 1H), 1.49 (t, $J = 4.4$ Hz, 1H); IR (film) ν_{max} 3318, 3048, 1591 1245 cm^{-1}; HRMALDI-FTMS (DHB) *m/z* 300.1381 (M+H$^+$, $C_{21}H_{17}NO$ requires 300.1383). Natural-**16**: $[\alpha]_D^{23}$ +160 (*c* 0.20, acetone); *ent*-**16**: $[\alpha]_D^{23}$ −163 (*c* 0.20, acetone).

4.12. *N*-(*E*-2-(4-Nitrophenyl)-1-ethenyl)-1,2,9,9a-tetrahydropropa[*c*]benz[*e*]indol-4-one (17)

A mixture of CBI (3.9 mg, 20 μmol), 2-(*E*-2-bromo-1-ethenyl)-4-nitrobenzene (4.7 mg, 21 μmol), Cs_2CO_3 (10.3 mg, 32 μmol), $Pd_2(dba)_3$ (0.9 mg, 1 μmol), and 2-dicyclohexylphosphino-2′-(*N*,*N*-dimethylamino)-biphenyl (0.8 mg, 2 μmol) under Ar was treated with THF (200 μL) and warmed at reflux for 10 h. The reaction mixture was diluted with EtOAc (30 mL), washed with saturated aqueous NH_4Cl (1×10 mL), dried (Na_2SO_4), and concentrated. PTLC (SiO_2, 20×20 cm, 50% EtOAc–hexanes) afforded **17** (2.0 mg, 36%) as a red film: ^{1}H NMR (acetone-d_6, 400 MHz) δ 8.13 (d, $J = 7.0$ Hz, 2H), 8.07 (dd, $J = 7.9$, 1.0 Hz, 1H), 7.89 (d, $J = 14.4$ Hz, 1H), 7.76 (d, $J = 9.0$ Hz, 2H), 7.51 (dt, $J = 7.5$, 1.5 Hz, 1H), 7.38 (dt, $J = 7.8$, 1.2 Hz, 1H), 7.11 (d, $J = 7.8$ Hz, 1H), 6.22 (s, 1H), 6.18 (d, $J = 14.2$ Hz, 1H), 4.14 (dd, $J = 10.9$, 5.2 Hz, 1H), 4.03

(d, $J = 10.7$ Hz, 1H), 3.21 (m, 1H), 1.70 (dd, $J = 7.8$, 4.2 Hz, 1H), 1.54 (t, $J = 4.5$ Hz, 1H); IR (film) ν_{max} 2919, 1590, 1314 cm^{-1}; HRMALDI-FTMS (DHB) *m/z* 345.1238 ($M+H^+$, $C_{21}H_{16}N_2O_3$ requires 345.1234). Natural-**17**: $[\alpha]_D^{23}$ +150 (*c* 0.05, THF); *ent*-**17**: $[\alpha]_D^{23}$ −160 (*c* 0.05, THF).

4.13. *N*-(*E*-2-(3,4,5-Trimethoxyphenyl)-1-ethenyl)-1,2,9,9a-tetrahydropropa[*c*]benz[*e*]indol-4-one (18)

A mixture of CBI (4.9 mg, 25 μmol), 2-(*E*-2-bromo-1-ethenyl)-3,4,5-trimethoxybenzene (8.2 mg, 30 μmol), Cs_2CO_3 (9.7 mg, 30 μmol), $Pd_2(dba)_3$ (1.1 mg, 1.3 μmol), and 2-dicyclohexylphosphino-2′-(*N*,*N*-dimethylamino)-biphenyl (1.0 mg, 2.5 μmol) under Ar was treated with DME (150 μL) and warmed at reflux for 6 h. The reaction mixture was diluted with EtOAc (30 mL), washed with saturated aqueous NH_4Cl (1 × 10 mL), dried (Na_2SO_4), and concentrated. Flash chromatography (SiO_2, 1 × 10 cm, 10–50% EtOAc–hexanes) afforded **18** (1.9 mg, 20%) as an off-white film: ^1H NMR (acetone-d_6, 400 MHz) δ 8.06 (dd, $J = 7.8$, 1.0 Hz, 1H), 7.48 (d, $J = 14.2$ Hz, 1H), 7.46 (d, $J = 6.6$ Hz, 1H), 7.08 (d, $J = 7.8$ Hz, 1H), 6.82 (s, 2H), 6.02 (d, $J = 14.2$ Hz, 1H), 5.98 (s, 1H), 4.08 (dd, $J = 10.6$, 5.2 Hz, 1H), 3.95 (d, $J = 10.8$ Hz, 1H), 3.84 (s, 6H), 3.70 (s, 3H), 3.15 (m, 1H), 1.65 (dd, $J = 7.8$, 4.0 Hz, 1H), 1.47 (t, $J = 4.4$ Hz, 1H); IR (film) ν_{max} 2919, 2849, 1596 cm^{-1}; HRMALDI-FTMS (DHB) *m/z* 412.1508 ($M+Na^+$, $C_{24}H_{23}NO_4$ requires 412,1519). Natural-**18**: $[\alpha]_D^{23}$ +60 (*c* 0.02, THF); *ent*-**18**: $[\alpha]_D^{23}$ −70 (*c* 0.02, THF).

4.14. *N*-(*E*-2-(2,3,4-Trimethoxyphenyl)-1-ethenyl)-1,2,9,9a-tetrahydropropa[*c*]benz[*e*]indol-4-one (19)

A mixture of CBI (3.9 mg, 20 μmol), (*E*)-1-(2-bromo-ethenyl)-2,3,4-trimethoxybenzene (5.7 mg, 21 μmol), Cs_2CO_3 (10.3 mg, 32 μmol), $Pd_2(dba)_3$ (0.9 mg, 1 μmol), and 2-dicyclohexylphosphino-2′-(*N*,*N*-dimethylamino)-biphenyl (0.8 mg, 2 μmol) under Ar was treated with THF (200 μL) and warmed at reflux for 6 h. The reaction mixture was diluted with EtOAc (30 mL), washed with saturated aqueous NH_4Cl (1 × 10 mL), dried (Na_2SO_4), and concentrated. PTLC (SiO_2, 10 × 20 cm, 50% EtOAc–hexanes) afforded **19** (3.3 mg, 43%) as an off-white film, which was determined to be an *E*/*Z* mixture (40/60) by ^1H NMR. A solution of **19** in 10% aqueous THF (4 mL) was stirred with SiO_2 (1 g) for 21 d at 25 °C (at which time ^1H NMR analysis of the reaction mixture indicated that only the *E*-isomer of **19** was present). The suspension was then filtered and concentrated. PTLC (SiO_2, 10 × 20 cm, 50% EtOAc–hexanes) afforded **19** (1.9 mg, 25%) as an off-white film: ^1H NMR (acetone-d_6, 400 MHz) δ 8.07 (d, $J = 7.8$ Hz, 1H), 7.48 (app t, $J = 8.7$ Hz, 1H), 7.45 (d, $J = 14.4$ Hz, 1H), 7.35 (app t, $J = 7.8$ Hz, 1H), 7.33 (d, $J = 8.8$ Hz, 1H), 7.08 (d, $J = 7.6$ Hz, 1H), 6.76 (d, $J = 8.8$ Hz, 1H), 6.13 (d, $J = 14.5$ Hz, 1H), 5.95 (s, 1H), 4.10 (dd, $J = 10.7$, 5.2 Hz, 1H), 3.96 (d, $J = 10.7$ Hz, 1H), 3.84 (s, 6H), 3.79 (s, 3H), 3.15 (m, 1H), 1.66 (dd, $J = 7.8$, 4.0 Hz, 1H), 1.47 (t, $J = 4.4$ Hz, 1H); IR (film) ν_{max} 2908, 2849, 1596 cm^{-1}; HRMALDI-FTMS (DHB) *m/z* 390.1695 ($M+H^+$, $C_{24}H_{23}NO_4$ requires 390.1705). Natural-**19**: $[\alpha]_D^{23}$ −50 (*c* 0.02, THF); *ent*-**19**: $[\alpha]_D^{23}$ +40 (*c* 0.02, THF).

4.15. *N*-(*E*-2-(1-Methyl-5,6,7-trimethoxy-2-indolyl)-1-ethenyl)-1,2,9,9a-tetrahydropropa[*c*]benz[*e*]indol-4-one (20)

A mixture of CBI (4.4 mg, 22 μmol), (*E*)-1-(2-bromo-ethenyl)-5,6,7-trimethoxy-1-methyl-1*H*-indole (10.9 mg, 34 μmol), Cs_2CO_3 (11.6 mg, 36 μmol), $Pd_2(dba)_3$ (1.0 mg, 1 μmol), and 2-dicyclohexylphosphino-2′-(*N*,*N*-dimethylamino)biphenyl (0.9 mg, 2 μmol) under Ar was treated with THF (220 μL) and warmed at reflux for 5 h. The reaction mixture was diluted with EtOAc (30 mL), washed with saturated aqueous NH_4Cl (1 × 10 mL), dried (Na_2SO_4), and concentrated. PTLC (SiO_2, 10 × 20 cm, 50% EtOAc–hexanes) afforded **20** (3.2 mg, 32%) as an orange solid: ^1H NMR (acetone-d_6, 400 MHz) δ 8.07 (dd, $J = 7.8$, 1.0 Hz, 1H), 7.47 (m, 2H), 7.09 (d, $J = 7.4$ Hz, 1H), 6.76 (s, 1H), 6.61 (s, 1H), 6.11 (d, $J = 14.0$ Hz, 1H), 6.03 (s, 1H), 4.15 (dd, $J = 10.8$, 5.3 Hz, 1H), 4.03 (d, $J = 10.8$ Hz, 1H), 3.94 (s, 6H), 3.81 (s, 3H), 3.80 (s, 3H), 3.18 (m, 1H), 1.68 (dd, $J = 7.8$, 4.1 Hz, 1H), 1.51 (t, $J = 4.5$ Hz, 1H); IR (film) ν_{max} 2919, 1596 cm^{-1}; HRMALDI-FTMS (DHB) *m/z* 443.1973 ($M+H^+$, $C_{27}H_{26}N_2O_4$ requires 443.1965). Natural-**20**: $[\alpha]_D^{23}$ +180 (*c* 0.10, THF); *ent*-**20**: $[\alpha]_D^{23}$ −175 (*c* 0.10, THF).

4.16. Addition of HCl to 9: *N*-phenyl-1-(chloromethyl)-5-hydroxy-1,2-dihydro-3*H*-benz[*e*]indole (21)

A solution of **9** (1.7 mg, 6.2 μmol) in THF (50 μL) was treated with 4 N HCl–EtOAc (50 μL) at room temperature under Ar. The mixture was stirred for 3 h before the solvent was removed in vacuo. PTLC (SiO_2, 10 × 10 cm, 50% EtOAc–hexanes) afforded **21** (1.7 mg, 88%) as a gray solid: $R_f = 0.55$ (50% EtOAc–hexanes); ^1H NMR (acetone-d_6, 500 MHz) δ 8.64 (s, 1H), 8.10 (d, $J = 8.5$ Hz, 1H), 7.72 (d, $J = 8.5$ Hz, 1H), 7.48 (m, 2H), 7.38 (app t, $J = 8.0$ Hz, 2H), 7.27 (m, 2H), 7.14 (t, $J = 7.4$ Hz, 1H), 6.44 (s, 1H), 4.74 (m, 1H), 4.05 (d, $J = 11.0$ Hz, 1H), 3.80 (dd, $J = 7.7$, 4.8 Hz, 1H), 3.63 (m, 1H), 3.25 (m, 1H); HRMALDI-FTMS (DHB) *m/z* 310.0996 ($M+H^+$, $C_{19}H_{17}ClNO$ requires 310.0993).

4.17. Acid-catalyzed addition of CH_3OH to 9: *N*-phenyl-1-(methoxymethyl)-5-hydroxy-1,2-dihydro-3*H*-benz[e]indole (22)

A solution of **9** (4.8 mg, 17.6 μmol) in anhydrous CH_3OH (1.0 mL) was treated with 0.02 M CF_3SO_3H–MeOH (105 μL, 2.10 μmol) at 0 °C. The reaction mixture was stirred for 12 h before being quenched by the addition of $NaHCO_3$ (2.0 mg), filtered through Celite, and concentrated in vacuo. PTLC (SiO_2, 10 × 20 cm, 17% EtOAc–hexanes) afforded recovered starting material (4.2 mg, 88%) and **22** (600 μg, 11%) as a yellow solid: $R_f = 0.69$ (17% EtOAc–hexanes); ^1H NMR ($CDCl_3$, 600 MHz) δ 8.14 (d, $J = 7.0$ Hz, 1H), 7.57 (m, 2H), 7.49 (dd, $J = 7.9$, 7.0 Hz, 1H), 7.44 (m, 3H), 7.36 (d, $J = 7.5$ Hz, 2H), 5.84 (s, 1H), 4.46 (m, 1H), 4.09 (d, $J = 10.1$ Hz, 1H), 3.51 (m, 1H), 3.36 (m, 1H), 3.22 (s,

3H), 2.96 (t, $J = 10.1$ Hz, 2H); IR (film) ν_{max} 3306, 2924, 2855, 1616, 1590, 1555, 1494, 1271, 1101 cm^{-1}; HRMALDI-FTMS (DHB) *m/z* 306.1486 ($M+H^+$, $C_{20}H_{20}NO_2$ requires 306.1488).

4.18. Aqueous solvolysis reactivity: pH 2

Compounds **6–15** (50 μg) were dissolved in CH_3OH (1.5 mL) and mixed with pH 2 aqueous buffer (1.5 mL). The buffer contained 4:1:20 (v:v:v) 1.0 M citric acid, 0.2 M Na_2HPO_4, and H_2O, respectively. Immediately after mixing, the UV spectra of the solutions was measured against a reference solution containing CH_3OH (1.5 mL) and the aqueous buffer (1.5 mL), and these readings were used as the initial absorbance values. The solutions were stoppered, protected from light, and allowed to stand at 25 °C. UV spectra were recorded at regular intervals until constant values were obtained for the long-wavelength absorbances. The solvolysis rate constants were determined from the slope of the line obtained from the linear least-squares treatment of the plot of $\ln[(A_f - A_i)/(A_f - A)]$ versus time using the long-wavelength measurements for **6–15**. The first order rate constants determined under these conditions are shown in Table 2.

4.19. DNA alkylation studies

The DNA alkylation experiments were conducted using experimental protocols previously described in detail[21] enlisting conditions described in the Figure 5 legend.

4.20. Cytotoxic activity

The L1210 cytotoxic assays were conducted as detailed previously[12] and the IC_{50} values reported represent the average of 2–7 determinations conducted in triplicate.

Acknowledgements

We gratefully acknowledge the financial support of NIH (CA41986) and the Skaggs Institute for Chemical Biology. We thank the American Society for Engineering Education (NDSEG) for a predoctoral fellowship (J.D.T.). We especially thank Dr. R. Chadha for the X-ray structure determinations.

Supporting data

Supplementary data associated with this article can be found, in the online version, at doi:10.1016/j.bmc.2004.08.032. ^1H NMR spectra of **6–22** and data for the *N*-acyl alkylation subunit analogues used for Figures 7,8 is provided. This material is available free of charge and via the Internet at http://pubs.acs.org.

References and notes

1. Chidester, C. G.; Krueger, W. C.; Mizsak, S. A.; Duchamp, D. J.; Martin, D. G. *J. Am. Chem. Soc.* **1981**, *103*, 7629.
2. Takahashi, I.; Takahashi, K.; Ichimura, M.; Morimoto, M.; Asano, K.; Kawamoto, I.; Tomita, F.; Nakano, H. *J. Antibiot.* **1988**, *41*, 1915.
3. Ichimura, M.; Ogawa, T.; Takahashi, K.; Kobayashi, E.; Kawamoto, I.; Yasuzawa, T.; Takahashi, I.; Nakano, H. *J. Antibiot.* **1990**, *43*, 1037; Yasuzawa, T.; Muroi, K.; Ichimura, M.; Takahashi, I.; Ogawa, T.; Takahashi, K.; Sano, H.; Saitoh, Y. *Chem. Pharm. Bull.* **1995**, *43*, 378.
4. Igarashi, Y.; Futamata, K.; Fujita, T.; Sekine, A.; Senda, H.; Naoki, H.; Furumai, T. *J. Antibiot.* **2003**, *56*, 107; Structure revision: Tichenor, M. S.; Kastrinsky, D. B.; Boger, D. L. *J. Am. Chem. Soc.* **2004**, *126*, 8396–8398.
5. Boger, D. L.; Johnson, D. S. *Angew. Chem., Int. Ed.* **1996**, *35*, 1438; For earlier reviews, see: Boger, D. L. *Acc. Chem. Res.* **1995**, *28*, 20; Boger, D. L.; Johnson, D. S. *Proc. Natl. Acad. Sci. U.S.A.* **1995**, *92*, 3642; Boger, D. L. *Chemtracts: Org. Chem.* **1991**, *4*, 329.
6. Warpehoski, M. A.; Hurley, L. H. *Chem. Res. Toxicol.* **1988**, *1*, 315.
7. Parrish, J. P.; Kastrinsky, D. B.; Wolkenberg, S. E.; Igarashi, Y.; Boger, D. L. *J. Am. Chem. Soc.* **2003**, *125*, 10971.
8. Boger, D. L.; Garbaccio, R. M. *Bioorg. Med. Chem.* **1997**, *5*, 263.
9. Boger, D. L.; Garbaccio, R. M. *Acc. Chem. Res.* **1999**, *32*, 1043.
10. Wolkenberg, S. E.; Boger, D. L. *Chem. Rev.* **2002**, *102*, 2477.
11. Boger, D. L.; Boyce, C. W.; Garbaccio, R. M.; Goldberg, J. *Chem. Rev.* **1997**, *97*, 787.
12. (a) Boger, D. L.; Ishizaki, T.; Kitos, P. A.; Suntornwat, O. *J. Org. Chem.* **1990**, *55*, 5823; (b) Parrish, J. P.; Kastrinsky, D. B.; Stauffer, F.; Hedrick, M. P.; Hwang, I.; Boger, D. L. *Bioorg. Med. Chem.* **2003**, *11*, 3815, and references cited therein.
13. Parrish, J. P.; Hughes, T. V.; Hwang, I.; Boger, D. L. *J. Am. Chem. Soc.* **2004**, *126*, 80.
14. Louie, J.; Hartwig, J. F. *Tetrahedron Lett.* **1995**, *36*, 3609; Guram, A. S.; Rennels, R. A.; Buchwald, S. L. *Angew. Chem., Int. Ed. Engl.* **1995**, *34*, 1348.
15. Barton, D. H. R.; Finet, J.-P.; Khamsi, J. *Tetrahedron Lett.* **1987**, *28*, 887; Review: Elliott, G. I.; Konopelski, J. P. *Tetrahedron* **2001**, *57*, 5683.
16. $(Cy)_2P$(DMAbp) = 2-Dicyclohexylphosphino-2′-(*N*,*N*-dimethylamino)biphenyl: Tomori, H.; Fox, J. M.; Buchwald, S. L. *J. Org. Chem.* **2000**, *65*, 5334.
17. Prepared by treatment of corresponding aryl bromide (1.0 equiv) with *n*-BuLi (1.1 equiv) in THF at −78 °C for 1 h, followed by addition of a THF solution of $BiCl_3$ (0.33 equiv). Solvent removal and recrystallization from toluene afforded pure Ar_3Bi. See: Hassan, A.; Breeze, S. R.; Courtenay, S.; Deslippe, C.; Wang, S. *Organometallics* **1996**, *15*, 5614.
18. Corey, E. J.; Fuchs, P. L. *Tetrahedron Lett.* **1972**, *36*, 3769.
19. Hirao, T.; Masunaga, T.; Ohshiro, Y.; Agawa, T. *J. Org. Chem.* **1981**, *46*, 374; Kuang, C.; Senboku, H.; Tokuda, M. *Synlett* **2000**, *10*, 1439; Uenishi, J.; Kawahama, A.; Yonemitsu, O.; Tsuji, J. *J. Org. Chem.* **1998**, *63*, 8965; Herz, H.-G.; Queiroz, M. J. R. P.; Maas, G. *Synthesis* **1999**, *6*, 1013.
20. The X-ray structures have been deposited with the Cambridge Crystallographic Data Centre: **7** (CCDC 216387), **8** (CCDC 216389), **9** (CCDC 216392), **10** (CCDC 216388), **11** (CCDC 216391), **12** (CCDC 216385), **13** (CCDC 216386), and **14** (CCDC 216390).
21. Boger, D. L.; Munk, S. A.; Zarrinmayeh, H.; Ishizaki, T.; Haught, J.; Bina, M. *Tetrahedron* **1991**, *47*, 2661.
22. Boger, D. L.; Munk, S. A.; Ishizaki, T. *J. Am. Chem. Soc.* **1991**, *113*, 2779.

23. Boger, D. L.; Johnson, D. S.; Yun, W. J. *J. Am. Chem. Soc.* **1994**, *116*, 1635.
24. Boger, D. L.; Santillán, A., Jr.; Searcey, M.; Jin, Q. *J. Am. Chem. Soc.* **1998**, *120*, 11554; Boger, D. L.; Santillán, A., Jr.; Searcey, M.; Jin, Q. *J. Org. Chem.* **1999**, *64*, 5241.
25. Boger, D. L.; Ishizaki, T. *Tetrahedron Lett.* **1990**, *31*, 793; Boger, D. L.; Yun, W. *J. Am. Chem. Soc.* **1994**, *116*, 5523; Boger, D. L.; Yun, W. *J. Am. Chem. Soc.* **1994**, *116*, 7996.
26. Exceptions have been noted and typically constitute unreactive derivatives (too stable) that fail to alkylate DNA (not active). These now may be fit onto the parabolic relationships described herein, see: Ref. 24 and Castedo, L.; Delamano, J.; Enjo, J.; Fernandez, J.; Gravalos, D. G.; Leis, R.; Lopez, C.; Marcos, C. F.; Rios, A.; Tojo, G. *J. Am. Chem. Soc.* **2001**, *123*, 5102.
27. References, and data for these compounds are provided in Supplementary material.